4D Motion Modeling of the Coronary Arteries from CT Images for Robotic Assisted Minimally Invasive Surgery

Dong Ping Zhang[1], Eddie Edwards[1,2], Lin Mei[1,2], Daniel Rueckert[1]

[1] Department of Computing, Imperial College London, UK

[2] Department of Biosurgery and Surgical Technology, Imperial College London, UK

ABSTRACT

In this paper, we present a novel approach for coronary artery motion modeling from cardiac Computed Tomography(CT) images. The aim of this work is to develop a 4D motion model of the coronaries for image guidance in robotic-assisted totally endoscopic coronary artery bypass (TECAB) surgery. To utilize the pre-operative cardiac images to guide the minimally invasive surgery, it is essential to have a 4D cardiac motion model to be registered with the stereo endoscopic images acquired intraoperatively using the da Vinci robotic system. In this paper, we are investigating the extraction of the coronary arteries and the modelling of their motion from a dynamic sequence of cardiac CT. We use a multi-scale vesselness filter to enhance vessels in the cardiac CT images. The centerlines of the arteries are extracted using a ridge traversal algorithm. Using this method the coronaries can be extracted in near real-time as only local information is used in vessel tracking. To compute the deformation of the coronaries due to cardiac motion, the motion is extracted from a dynamic sequence of cardiac CT. Each timeframe in this sequence is registered to the end-diastole timeframe of the sequence using a non-rigid registration algorithm based on free-form deformations. Once the images have been registered a dynamic motion model of the coronaries can be obtained by applying the computed free-form deformations to the extracted coronary arteries. To validate the accuracy of the motion model we compare the actual position of the coronaries in each time frame with the predicted position of the coronaries as estimated from the non-rigid registration. We expect that this motion model of coronaries can facilitate the planning of TECAB surgery, and through the registration with real-time endoscopic video images it can reduce the conversion rate from TECAB to conventional procedures.

Keywords: Image-Guided Therapy, Motion Analysis, Registration, Segmentation, Vascular Analysis

1. INTRODUCTION

1.1 Purpose

As the most common cause of heart disease, coronary artery disease is the leading cause of sudden death in the western world. Conventional bypass surgery requires invasive sternotomy and the use of a cardiopulmonary bypass, which leads to long recovery period and has high infectious potential. Totally endoscopic coronary artery bypass (TECAB) surgery based on image guided robotic surgical approaches have been developed to allow the clinicians to conduct the bypass surgery off-pump with only three pin holes incisions in the chest cavity, through which two robotic arms and one stereo endoscopic camera are inserted. Figure 1 shows the endoscopic views taken during the TECAB surgery, with the operating instruments present.

However, the restricted field of view of the stereo endoscopic images, possible vessel misidentification and coronary artery mis-localization can cause relatively high conversion rates from TECAB surgery to the conventional invasive surgical approach.[1]

An prototype image-guided TECAB system has been recently developed by M. Figl et al previously.[2] The system requires a 4D preoperative model of the coronary arteries and myocardium which is then aligned with the endoscopic view of the patient's beating heart. This allows the superimposition of structures of interest such as the coronary using augmented reality on top of the endoscopic video. The work presented in this paper focuses on the 4D model construction part in the system.

In this paper we present a fast and accurate method for extracting coronary centerlines and tracking its motion from 3D preoperative Computed Tomography image sequences. We aim to construct patient-specific 3D

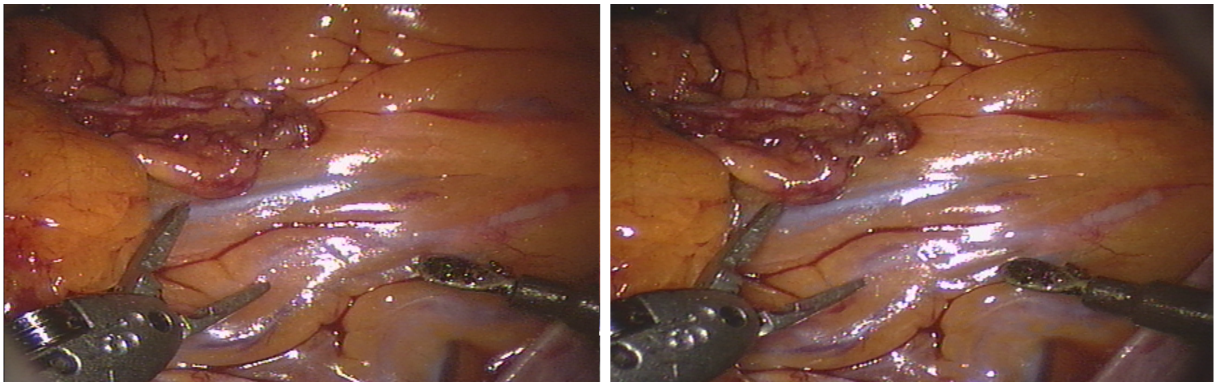

Figure 1. Endoscopic stereo views (left and right) of the coronary arteries during the TECAB surgery.

+ time coronary artery motion models from preoperative CT images. Through temporally and spatially aligning this model with the intraoperative endoscopic video images, we hope this work can assist surgical planning and help conducting the TECAB surgery.

1.2 Related Work

The extraction of blood vessel has been studied extensively in the past two decades. Previous research on vessel extraction has been concentrated on 2D X-ray angiography, 3D Magnetic Resonance Angiography (MRA) and Computed Tomography Angiography (CTA), focusing on brain and cardiac images. A comprehensive review about vessel extraction can be found in Kirbas et al.[3]

Various vessel enhancement techniques have been proposed in last decade. Three of the post popular techniques for curvilinear structure filtering are presented by Frangi et al. ,[4] Lorenz et al. [5] and Sato et al. [6] All of these approaches are based on extracting information from the second order intensity derivatives at multiple scales to identify local structures in the images. Based in the information it is possible to classify the local intensity structure as tubular-like, sheet-like or blob-like.

Existing vessel extraction methods can broadly be divided into two categories: skeleton and non-skeleton approaches. Skeleton methods explicitly extract the vessel centerlines and represent the results as parametric curves or discrete sets of points. Two main skeleton methods are closely related to the work we present: Frangi et al. [7] propose a model-based method using a deformable contour techniques. A central vessel axis curve coupled with a tensor product B-spline surface is used to model the linear vessel segments. In this approach the vessel centerline is approximated using a B-spline curve. The deformation process is based on moving the control points of B-spline towards points which have a high likelihood of lying along the central vessel axis. A vesselness filter is used as the external force which drives the deformation. The vesselness filter reaches its maximum at the center of the vessel and explicitly takes information of vessel radius into account. Secondly, a tensor product B-spline surface is used to model the vessel wall. Based on the observation that vessel centerlines often corresponds to intensity ridge in the TOF-MRA images, Aylward and Bullitt [8] propose a ridge travsersal algorithm to track the vessel centerlines. This method begins from a user-supplied seed point, then optimizing a pre-defined ridgeness function to obtain the closest local ridge point.

Many methods have also been developed for the extraction of cardiac motion from dynamic image sequences such as CT or MR. Optical flow,[9] active contour models,[10] HARP [11] and image registration approaches.[12] Compared with other methods which rely on specialized image sequences such as tagged MR or HARP, non-rigid image registration based on voxel similarity measures does not require any explicit feature extraction and can be used on both MR and CT images. Moreover, given different types of images, the voxel similarity measure can be chosen to calculate a suitable metric for that particular type of images. For cardiac motion tracking, non-rigid registration based on a free-form deformation (FFD) model has shown promising results in previous work presented by Chandrashekara et al.[13]

2. METHODS

A 4D motion model of the beating heart with coronary arteries is needed for guiding the TECAB procedure. This is achieved by extracting the vessel centerlines from the end-diastole time frame of the CT image sequence, aligning the sequence of cardiac CT images to the end-diastole time frame, and applying the deformation to the extracted coronaries at end-diastole. The resulting patient-specific motion model can then be used to augment the intraoperative images acquired with stereo-endoscope of the daVinci robot.

2.1 Coronary Artery Extraction

The CT images are first processed with a multiscale Hessian-based vessel enhancement filter.[7] The filter utilizes the 2nd-order derivatives of the image intensity at multiple scales to identify bright tubular-like structures. The maximum response of this filter over a set of different scales is collected to provide a coarse segmentation of the coronary arteries. The vesselness of each voxel is computed from the analysis of the Hessian matrix of second derivatives in the local area after convolving with Gaussian kernel at pre-selected scale value.

Assuming a continuous image function $I(p)$, $p = (x, y, z)$, the Hessian matrix for the 3D image at any point p is defined as:

$$H(\mathrm{p}) = \begin{bmatrix} \frac{\partial^2 I(p)}{\partial x \partial x} & \frac{\partial^2 I(p)}{\partial x \partial y} & \frac{\partial^2 I(p)}{\partial x \partial z} \\ \frac{\partial^2 I(p)}{\partial x \partial y} & \frac{\partial^2 I(p)}{\partial y \partial y} & \frac{\partial^2 I(p)}{\partial y \partial z} \\ \frac{\partial^2 I(p)}{\partial x \partial z} & \frac{\partial^2 I(p)}{\partial y \partial z} & \frac{\partial^2 I(p)}{\partial z \partial z} \end{bmatrix} \tag{1}$$

Let $|\lambda_1| > |\lambda_2| > |\lambda_3|$ denote the eigenvalues of the Hessian matrix and $\vec{v_1}$,$\vec{v_2}$,$\vec{v_3}$ are the corresponding eigenvectors. The principal curvature directions are then given by $\vec{v_1}$ and $\vec{v_2}$.

Since vessels have higher intensity in CT images than soft tissues, one can define vessels in terms of intensity ridges. For n-dimensional image ridge points can be defined as points which are local intensity maxima in $N-1$ dimensions. Thus, for a 3D image the corresponding eigenvalues λ_1 and λ_2 for ridge points should be negative:

$$\lambda_1 < 0 \tag{2}$$

$$\lambda_2 < 0 \tag{3}$$

We use the vesselness definition at scale σ as proposed by Frangi et al. [7]

$$v(\sigma) = \begin{cases} 0 \quad if\ \lambda_1 > 0 \quad else \\ \left(1 - exp\left(-\frac{A^2}{2\alpha^2}\right)\right) exp\left(-\frac{B^2}{2\beta^2}\right)\left(1 - exp\left(-\frac{S^2}{2\gamma^2}\right)\right) \end{cases} \tag{4}$$

where

$$A = \frac{|\lambda_1|}{|\lambda_2|}$$

$$B = \frac{|\lambda_1|}{\sqrt{|\lambda_2 \lambda_3|}}$$

$$S = \sqrt{\lambda_1^2 + \lambda_2^2 + \lambda_3^2}$$

The parameter A distinguishes between the plate-like and line-like structures. The parameter B reflects the deviation from blob-like structure and parameter S differentiates regions with high contrast from low contrast background. The parameters α, β, γ control the sensitivity of the tubular filter to A, B and C in the above equation.

For parameter selections, we refer to Lindeberg et al.[14] In our experiments, we set the parameters $\alpha = 0.5$, $\beta = 0.5$, $\gamma = 1$. The vesselness response is computed at different scales, namely $\sigma = 0.25, 0.5, 1, 2, 4, 8$. The maximum response with corresponding optimal scale is obtained for each voxel of the image. The calculated vesselness image is used to facilitate the identification of coronaries.

2.2 Cardiac Motion Extraction by Image Registration

The motion of the heart is obtained from non-rigid image registration using a free-form deformation model based on cubic B-splines.[15] In this approach the motion is modelled using the following model:

$$T(x, y, z) = \sum_{l=0}^{3}\sum_{m=0}^{3}\sum_{n=0}^{3} B_l(u)B_m(v)B_n(w)\phi_{i+l,j+m,k+n} \tag{5}$$

Here B_i corresponds to the cubic B-spline basis functions:

$$\begin{aligned}
B_0(u) &= (1-u)^3/6 \\
B_1(u) &= (3u^3 - 6u^2 + 4)/6 \\
B_2(u) &= (-3u^3 + 3u^2 + 3u + 1)/6 \\
B_3(u) &= u^3/6
\end{aligned}$$

The image at the end-diastole frame of the cardiac cycle is chosen as the target image. In our two datasets, the end-diastole is at 60% of the cardiac cycle. For simplicity, we refer to this as frame 60 in this paper. Each image from the rest of the image sequence $I_t(p)$ ($t = 00, 10, 20, 30, 40, 50, 70, 80, 90$) is chosen as the source image and temporally registered to the target image $I_{60}(p)$.

We evaluate and optimize four different similarity measures for this procedure, namely, sums of squared difference (SSD), cross correlation (CC), mutual information (MI) and normalized mutual information (NMI). A gradient descent optimization procedure is used to find the optimal deformation. From the results of the non-rigid image registration, we can determine the corresponding deformation T_t due to the cardiac motion in the CT datasets.

2.3 Modeling of Coronary Artery Motion and Assessment

The cardiac motion extracted above can be used to predict the motion of coronaries in every time frame. For this the coronaries extracted from end-diastole timeframe are transformed with the obtained deformation information T_t to each time frame to form the coronary motion model.

In order to assess the quality of the deformation model, the distance between the predicted centerline and the automatically extracted vessels of each time frame is measured to assess the accuracy of applying the whole cardiac motion to coronaries deformation. We define this distance as

$$D\,(S,\,R,\,T) \;=\; \frac{1}{N_s}\textstyle\sum_{i=1}^{Ns} \|v_i - l(v_i, T(R))\|_2 + \frac{1}{N_r}\textstyle\sum_{j=1}^{N_r} \|p_j - l(p_j, S))\|_2 \tag{6}$$

where S and R are the source and reference images which are being registered. N_s and N_r are the number of vertices representing vessel S and vessel R correspondingly. For each vertex $v_i \in S$, $l(v_i,\, T(R))$ calculates the closest vertex of v_i on the transformed vessel $T(R)$. Similarly, for each vertex $p_j \in T(R)$, $l(p_j,\, S)$ defines the closest vertex of p_j on the vessel S. We expect the coronary motion can be recovered from the cardiac and respiratory deformation obtained from free form registration.

3. RESULTS

3.1 Vessel Enhancement and Extraction

A volume rendering of preoperative cardiac CT image from patient dataset I is shown in Figure 2. The coronary arteries and myocardial surfaces are displayed in three views. From left to right, left circumflex artery and branchs (LCX), left anterior descending artery and a diagonal branch (LAD) and right coronary artery (RCA) are visible.

The automatically extracted 3D coronary centerlines from this volume are shown in Figure 3. The red line denotes the right coronary artery, the blue line denotes the left anterior descending and its branches and the blue line denotes the left circumflex artery and its branches.

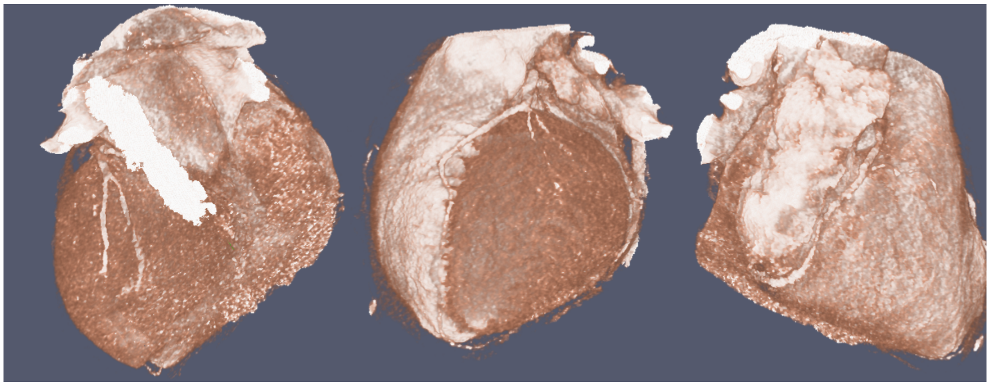

Figure 2. Volume rending of CT image in the end-diastolic time frame from patient dataset I.

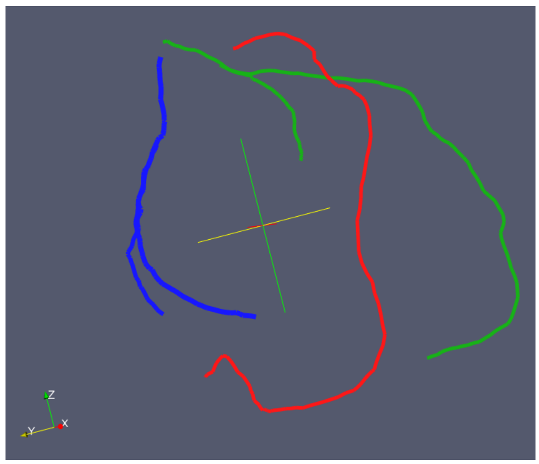

Figure 3. An extracted coronary model of the coronary centerlines. Red: right coronary artery, green: left anterior descending coronary artery and branch, blue: circumflex artery and branch.

3.2 Cardiac Motion Tracking

The deformation of the heart throughout the cardiac cycle from one patient dataset is illustrated in first two rows of Figure 4. The corresponding transformed image after alignment with reference (target) image is shown in the bottom two rows of Figure 4. Here we have used with the correlation coefficient to measure the similarity between the images.

3.3 Coronary Artery Motion Modelling

To evaluate the proposed approach, the coronary centerlines are extracted automatically from all images of the cardiac CT sequence. We then compare the predicted location of the centrelines obtained by applying the non-rigid deformation with the actual position of the centrelines.

The distance between the transformed vessel and extracted one in each time frame is measured using eq. 6. The current registration method can only recover part of the coronary motion. The reasons for this are two-fold: First, the image quality of dynamic cardiac CT is limited. This is especially true for CT image reconstructions during those times in the cardiac phase in which the heart moves rapidly. The second problem is the fact that the image registration is driven by large scale features such as the epicardium and endocardium. We are currently investigating better transformation and registration models to overcome these problems and improve the prediction of the coronary motions.

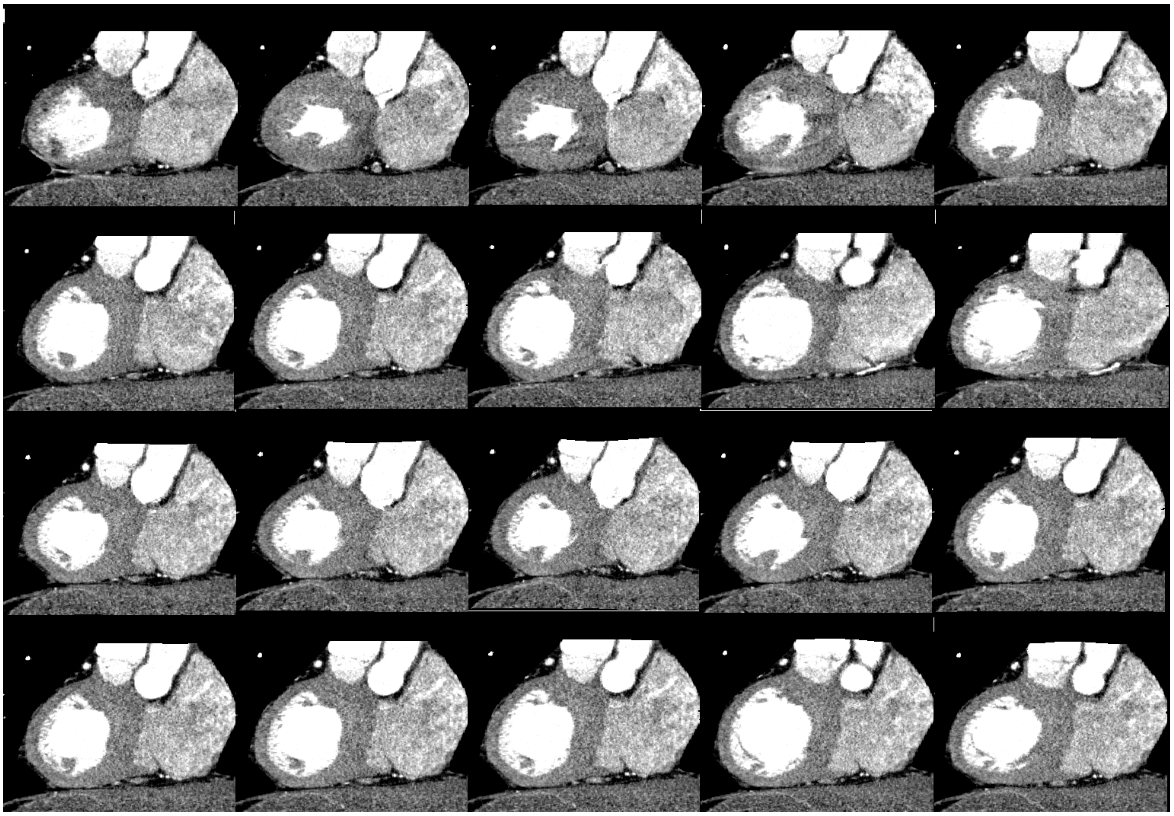

Figure 4. Example of 10 time fromes of a patient dataset before nonrigid registration shown in top two rows (from left to right, top to bottom sequentially) and afterwards (as shown in bottom two rows). The 2nd Frame in row 2 was chosen as the reference (target image).

4. DISCUSSION

Mourgues et al. [16] have proposed a method to reconstruct the 3D coronary tree from one pair of patient-specific biplane X-ray angiography images. Shechter et al. [17] have presented a motion tracking method for the coronary arteries from a temporal sequence of biplane X-ray angiograms. But to fully utilize the most common pre-operative patient data, we investigate the coronary vessel extraction and motion tracking from clinical coronary CT scans.

5. CONCLUSIONS

We have presented a novel approach for patient-specific coronary tree construction and motion modeling from CT images to assist the totally endoscopic coronary artery bypass surgery. The proposed method has been tested on the clinical CT datasets acquired from two subjects. By aligning the 4D coronary model with the series of 2D endoscopic images grabbed during the operation, we hope to assist the planning and conducting of TECAB surgery, and also reduce the conversion rate from TECAB to more invasive conventional procedures.

REFERENCES

1. F. W. Mohr, V. Falk, A. Diegeler, T. Walther, J. F. Gummert, J. Bucerius, S. Jacobs, and R. Autschbach, “Computer-enhanced ”robotic” cardiac surgery: Experience in 148 patients,” *Journal of Thoracic and Cardiovascular Surgery* **121**(5), pp. 842 – 853, 2001.
2. M. Figl, D. Rueckert, D. Hawkes, R. Casula, M. Hu, O. Pedro, D. P. Zhang, G. Penney, F. Bello, and P. Edwards, “Augmented reality image guidance for minimally invasive coronary artery bypass,” in *Proc. SPIE*, **6918**, pp. 69180P–69180P–7, 2008.

Dataset I frame No.	Distance before transformation	Distance after transformation	Dataset II frame No.	Distance before transformation	Distance after transformation
lad 00%	2.01	2.08	lad 00%	2.35	2.04
lad 10%	3.58	2.42	lad 10%	3.77	2.75
lad 20%	3.03	2.42	lad 20%	3.72	2.72
lad 30%	2.30	1.78	lad 30%	9.49	3.44
lad 40%	1.72	1.02	lad 40%	5.83	3.24
lad 50%	0.90	0.54	lad 50%	2.47	1.16
lad 60%	reference		lad 60%	reference	
lad 70%	0.84	0.46	lad 70%	1.88	0.52
lad 80%	1.26	0.97	lad 80%	2.09	1.02
lad 90%	2.03	1.66	lad 90%	2.68	1.73
lcx 00%	2.29	2.99	lcx 00%	1.66	1.55
lcx 10%	6.70	5.24	lcx 10%	14.89	0.73
lcx 20%	5.62	4.30	lcx 20%	14.07	2.78
lcx 30%	5.54	3.98	lcx 30%	10.63	3.56
lcx 40%	8.44	0.89	lcx 40%	8.55	3.72
lcx 50%	0.72	0.37	lcx 50%	4.28	1.08
lcx 60%	reference		lcx 60%	reference	
lcx 70%	1.58	0.66	lcx 70%	5.17	0.60
lcx 80%	4.23	3.25	lcx 80%	5.81	1.18
lcx 90%	4.86	3.96	lcx 90%	3.33	1.85
rca 00%	3.49	1.62	rca 00%	4.37	4.05
rca 10%	11.28	2.79	rca 10%	2.45	2.68
rca 20%	10.24	2.56	rca 20%	8.36	4.00
rca 30%	7.14	2.20	rca 30%	8.61	8.53
rca 40%	0.84	0.93	rca 40%	9.08	7.66
rca 50%	0.57	0.43	rca 50%	1.06	1.04
rca 60%	reference		rca 60%	reference	
rca 70%	3.78	0.32	rca 70%	1.63	1.45
rca 80%	9.65	1.81	rca 80%	2.01	1.87
rca 90%	8.60	1.79	rca 90%	14.43	3.95

Table 1. Distance between the centerline at end-diastole (60%) of cardiac cycle and the ones from other timeframes, for LAD, LCX, RCA (top to bottom). From left to right, the results from two patients datasets are examined.

3. C. Kirbas and F. Quek, "A review of vessel extraction techniques and algorithms," *ACM Computing Surveys* **36**(2), pp. 81–121, 2004.
4. A. F. Frangi, W. J. Niessen, K. L. Vincken, and M. A. Viergever, "Multiscale vessel enhancement filtering," in *Medical Image Computation and Computer-Assisted Intervention - MICCAI 98*, *Lecture Notes in Computer Science* **1496**, pp. 130–137, Springer, 1998.
5. C. Lorenz, I.-C. Carlsen, T. M. Buzug, C. Fassnacht, and J. Weese, "Multi-scale line segmentation with automatic estimation of width, contrast and tangential direction in 2D and 3D medical images," in *CVRMed-MRCAS '97: Proceedings of the First Joint Conference on Computer Vision, Virtual Reality and Robotics in Medicine and Medial Robotics and Computer-Assisted Surgery*, pp. 233–242, 1997.
6. Y. Sato, N. Shiraga, H. Atsumi, S. Yoshida, T. Koller, G. Gerig, and R. Kikinis, "Three-dimensional multi-scale line filter for segmentation and visualization of curvilinear structures in medical images," *Medical Image Analysis* **2**(2), pp. 143–168, 1998.
7. A. Frangi, W. Niessen, R. Hoogeveen, T. van Walsum, and M. Viergever, "Model-based quantitation of 3D magnetic resonance angiographic images," *IEEE Transactions on Medical Imaging* **18**(10), pp. 946–956, 1999.

8. S. Aylward and E. Bullitt, "Initialization, noise, singularities, and scale in height ridge traversal for tubular object centerline extraction," *IEEE Transactions on Medical Imaging* **21**, pp. 61–75, February 2002.
9. L. Dougherty, J. Asmuth, A. Blom, L. Axel, and R. Kumar, "Validation of an optical flow method for tag displacement estimation.," *IEEE Transactions on Medical Imaging* **18**(4), pp. 359–363, 1999.
10. W. O'Dell, C. Moore, W. Hunter, E. Zerhouni, and E. McVeigh, "Three-dimensional myocardial deformations: Calculation with displacement field fitting to tagged MRI images," *Radiology* **195**(3), pp. 829–835, 1995.
11. N. Osman, E. McVeigh, and J. Prince, "Imaging heart motion using harmonic phase MRI," *IEEE Transactions on Medical Imaging* **19**(3), pp. 186–202, 2000.
12. R. Chandrashekara, R. Mohiaddin, and D. Rueckert, "Analysis of 3D myocardial motion in tagged MR images using nonrigid image registration," *IEEE Transactions on Medical Imaging* **23**(10), pp. 1245–1250, 2004.
13. R. Chandrashekara, R. Mohiaddin, R. S. Razavi, and D. Rueckert, "Nonrigid image registration with subdivision lattices application to cardiac MR image analysis," in *Medical Image Computation and Computer-Assisted Intervention - MICCAI 2007*, *Lecture Notes in Computer Science* **4791**, pp. 335–342, Springer, 2007.
14. T. Lindeberg, "Feature detection with automatic scale selection," *International Journal of Computer Vision* **30**, pp. 79–116, 1998.
15. D. Rueckert, L. I. Sonoda, C. Hayes, D. L. Hill, M. O. Leach, and D. J. Hawkes, "Nonrigid registration using free-form deformations: application to breast MR images.," *IEEE Transactions on Medical Imaging* **18**(8), pp. 712–721, 1999.
16. F. Mourgues, F. Devernay, G. Malandain, and Ève Coste-Manière, "3D+t modeling of coronary artery tree from standard non simultaneous angiograms," in *Medical Image Computing and Computer-Assisted Intervention - MICCAI 2001*, *Lecture Notes in Computer Science* **2208/2008**, pp. 1320–1322, Springer, 2001.
17. G. Shechter, F. Devernay, A. Quyyumi, E. Coste-Maniere, and E. McVeigh, "Three-dimensional motion tracking of coronary arteries in biplane cineangiograms," *IEEE Transactions in Medical Imaging* **22(4)**, pp. 493–603, 2003.